(Mis)Measurement of Long-Horizon Default Risk: Debt Dynamics in Structural Models*

Söhnke M. Bartram† Peter Feldhütter‡ Dirk Hackbarth§ Yerkin Kitapbayev¶

March 17, 2026

Abstract

Structural credit risk models typically assume debt, and hence the default boundary, remains fixed over the default prediction horizon. This simplifying assumption becomes increasingly problematic at longer maturities, because firms refinance and adjust leverage over time. We develop a dynamic structural model in which refinancing endogenously shifts the default boundary upward and derive a tractable characterization of cumulative default probabilities over finite horizons via a Volterra integral equation. Relative to the conventional Black-Cox benchmark, the model implies a steeper term structure of default risk and shows that ignoring debt dynamics leads to an underestimation of long-horizon default probabilities. In a large panel of more than 2,000 U.S. firms from 1951 to 2023, refinancing-adjusted default probabilities match both the level and slope of realized default rates substantially better than the conventional model. The results identify debt dynamics as a first-order determinant of long-maturity default risk in structural credit risk models.

JEL Classification Numbers: C23, G12, G13, G23, G33.

Keywords: Credit Risk, Debt Restructuring, Default Boundaries, Default Rates, Structural Models.

*We are grateful to Marc Chesney, Darrel Duffie, Douglas Dwyer, Stephen Figlewski, Jens Hilscher, David Lando, Hayne Leland, Stephen Schaefer, Roger Stein, and Ilya Strebulaev for comments and suggestions.

†Research Fellow, Centre for Economic Policy Research (CEPR), London, UK, and Professor of Finance, University of Warwick, Warwick Business School, Finance Group, Coventry CV4 7AL, United Kingdom. Phone: +44 (24) 7657 4168, Fax: +1 (425) 952 10 70. Email: s.m.bartram@wbs.ac.uk. Webpage: http://go.warwick.ac.uk/sbartram.

‡Copenhagen Business School, Department of Finance, Denmark. Email: .

§Boston University, Questrom School of Business, USA. Email: dhackbar@bu.edu.

¶Department of Mathematics, Khalifa University, Abu Dhabi, United Arab Emirates. Email: yerkin.kitapbayev@ku.ac.ae.

1 Introduction

Default probabilities are used to price long-term corporate debt and to measure "distress risk" over horizons that matter for investors and researchers. Multi-year default probabilities are routinely summarized by a term structure: the probability a firm defaults within one, five, or ten years. In structural models of default, these probabilities are commonly computed under an implicit "passive-debt" assumption under which the default boundary remains constant over the prediction horizon. In practice, firms adjust outstanding debt levels in response to changes in firm value.

While the "passive debt" assumption delivers tractability, it also creates a systematic distortion in the term structure of default risk. Firms refinance, roll over liabilities, and adjust capital structure over time. If a firm's debt is instead assumed to remain constant while its asset value grows, financial leverage declines, implying default probabilities will be too low at longer horizons.[1] Therefore, a constant default boundary engenders mismeasurement that is compounded over time: most firms follow "active debt" policies and hence tend to return to leverage targets, changing the relevant default boundary routinely and making constant boundary models less suitable for generating longer term default probability predictions.

We extend a widely used class of structural default models to incorporate compelling debt dynamics and derives a tractable characterization of default probabilities under infrequent leverage adjustment through refinancing. We study a setting in which the firm defaults when its asset value falls to a lower boundary and refinances when its asset value rises to an upper boundary, so that future refinancing endogenously shifts the default boundary upward over time. We show that this mechanism generates a steeper term structure of default probabilities than the conventional Black-Cox model. Empirically, using a sample of more than 2,000 U.S. firms over 1951–2023, we find that the model with refinancing matches the observed term structure of default rates substantially better than the constant boundary benchmark: Model-implied default predictions are approximately twelve times more accurate than those of the Black-Cox model. These results reveal debt dynamics as a first-order determinant of long-maturity default risk in structural credit models.

[1] Alternatively, if a firm's asset value declines over time, its financial leverage rises over time. Both static debt scenarios are inconsistent with evidence on mean reversion in leverage ratios (Collin-Dufresne and Goldstein, 2001).

This paper bridges a gap between two important streams of research that have largely developed separately. One studies the dynamic capital structure and the endogenous decisions of firms about refinancing, default, and leverage adjustment over time (Fischer, Heinkel, and Zechner, 1989; Goldstein, Ju, and Leland, 2001; Strebulaev, 2007; Hackbarth, Miao, and Morellec, 2006; Chen, 2010; Bhamra, Kuehn, and Strebulaev, 2010). These infinite horizon models are economically rich, but they are less readily implemented for measuring default probabilities over finite horizons. The other one follows Merton (1974) and Black and Cox (1976) and provides analytically tractable default predictions that are widely used in empirical work and in practice (Eom, Helwege, and Huang, 2004; Huang and Huang, 2012; Feldhütter and Schaefer, 2018; Huang, Nozawa, and Shi, 2025). However, that tractability is generally obtained by abstracting from empirical regularities, such as mean reversion in leverage ratios.[2] Our contribution is to connect these heretofore separate literatures by including widely observed leverage targeting behavior in a default probability model in a way that remains analytically transparent, computationally feasible, and empirically implementable.

Our work makes several contributions to the literature. Our first contribution is theoretical. We derive cumulative default probabilities over finite horizons when the default boundary is no longer constant but evolves endogenously as firms refinance. This characterization relies on techniques from the pricing of double barrier options (Lin, 1998; Pelsser, 2000; Jeanblanc, Yor, and Chesney, 2006), which enables us to quantify how expected future debt issuance affects the term structure of default risk. By conditioning on the first refinancing time and exploiting the scaling structure of the model, we obtain a Volterra integral equation that characterizes default probabilities in the dynamic setting and that nests the Black-Cox formula as a special case in the absence of refinancing.[3] The methodology in this paper can be extended to debt renegotiation or restructuring rather than default when the firm's asset value declines to a lower boundary, thereby providing a tractable structural framework for incorporating realistic leverage patterns into default probability predictions.

Our second contribution is quantitative. We establish that expected future refinancing has im-

[2]Recently, Feldhütter and Schaefer (2018) point out that an important misspecification problem remains unresolved: "The fact that, on average, the face value of a firm's debt increases over time suggests that the Black-Cox model as we implement it is misspecified, because the model assumes that the default boundary is constant."

[3]For example, Volterra-type nonlinear integral equations have been used to characterize the optimal exercise boundary for finite maturity American options (Carr, Jarrow, and Myneni, 1992; Detemple, 2006).

portant implications for the measurement of credit risk. Our default probability formula generalizes the Black-Cox formula by allowing for refinancing in response to changes in a firm's asset value, and our comparison therefore isolates the importance of expected but uncertain future refinancing times on default probability predictions. Relative to the Black-Cox model, our model implies a steeper term structure of default probabilities, because it accounts for the possibility that refinancing raises the default boundary in the future. The comparison between the two models also clarifies why a model with a constant default boundary tends to understate default risk for longer horizons. Thus, allowing a firm to adjust its debt level in response to changes in firm value (i.e., following leverage tarrets) significantly changes default probability predictions.

Our third contribution is empirical. We evaluate the two default probability models using firm-level data for U.S. non-financial firms together with aggregate historical default rates and risk-free rates during the 1951–2023 period. The empirical implementation estimates the model parameters separately by rating category and compares average model-implied default term structures with historical default frequencies over horizons from one to twenty years. The key finding is that the default probability model with refinancing matches both the level and the slope of historical default rates substantially better than the Black-Cox model, especially at longer horizons, where the latter generates default probabilities that are too low. These results indicate that "active debt" policies are an important determinant of long-horizon default risk and help reconcile structural credit models with the observed term structure of default. Notably, our empirical results provide an explanation for why conventional structural models of credit risk mis-measure longer term default risk and suggest an economic mechanism—perhaps negligible at shorter horizons but certainly magnified by compounding at longer horizons—that alleviates the underlying mis-specification problem.

The remainder of the paper is organized as follows. Section 2 describes the debt dynamics implied by static and dynamic leverage policies and motivates the evolution of the default and refinancing boundaries. Section 3 derives default probabilities for the constant-boundary benchmark and for the dynamic refinancing model, and discusses numerical implementation and calibrated examples. Section 4 evaluates the model empirically against historical default rates. Section 5 concludes. Additional derivations are provided in the Appendix.

2 Debt Dynamics

To connect the literatures on leverage policies and default probabilities, we consider a simple setting for a firm's debt dynamics that assumes the firm's leverage policy follows from a commonly-used, continuous-time capital structure model with an initital (static) or a dynamic leverage target. Given that this setting has been used widely in recent research for both dynamic and static models of capital structure, we do not reproduce the solutions—see, e.g., Leland (1994), Goldstein, Ju, and Leland (2001), Hackbarth, Miao, and Morellec (2006), Strebulaev (2007), and many others. Importantly, we only need the models to 'discipline' inputs for default boundary values when comparing default probabilities in a calibrated example (see Subsection 3.5) and note that the inputs are also consistent with the data (see Section 4).

We consider a partial equilibrium model of corporate financing, in which time t is continuous and uncertainty is modeled by a complete probability space $(\Omega, \mathcal{F}, \mathbb{P})$. Under the actual probability measure $\mathbb{P}$, firm's asset value, $V(t)$, given a constant growth rate μ, a constant volatility σ, and an initial value $V(0) > 0$, evolves according to $dV(t)/V(t) = \mu\, dt + \sigma\, dW_t$ for $t > 0$. There is a constant, risk-free rate r, a constant tax rate τ, and the economy's pricing kernel, Λ_t, follows a geometric Brownian motion with volatility σ_Λ and correlation $\rho < 0$ with $V(t)$, characterizing the economy's risk-reward trade-off. Hence the risk-neutral drift is given by $\hat{\mu} = \mu + \rho\,\sigma\,\sigma_\Lambda$ and we assume $\hat{\mu} < r$. That is, under the physical measure $\mathbb{P}$, asset value $V(t)$ have a risk premium of $\pi = -\rho\,\sigma\,\sigma_\Lambda > 0$. The default probability requires the physical measure $\mathbb{P}$, but at the same time, all of the firm's optimal decisions are based on valuations under the risk-neutral measure $\mathbb{Q}$.

In the static version, the firm chooses an optimal capital structure of equity and perpetual, risky debt that balances tax benefits against bankruptcy and debt issuance costs. We consider debt contracts that are characterized by a perpetual flow of coupon payments c. The optimal time to default on coupon payments is endogenously determined (i.e. maximizes equity value). In the event of default, equityholders receive nothing and debtholders assume ownership of the firm's assets net of bankruptcy costs. Bankruptcy triggers a loss of interest tax shields and a fractional loss α of assets.

In the dynamic version, the firm can, for example, balance tax benefits against bankruptcy

and debt issuance costs at the initial date and at future restructuring dates. To stay in a simple time-homogeneous setting, debt is callable and issued at par. The proceeds from the debt issue are distributed on a pro rata basis to shareholders at the time of flotation. The firm can adjust their capital structure upwards at any point in time by incurring a proportional cost q, but they can reduce their indebtedness only in default. Under this assumption, the firm's initial debt level remains fixed until either the firm goes into default or the firm calls its debt and restructures with newly issued debt.That is, the firm selects a target leverage and infrequently returns to its target leverage unless default occurs.

This setting enables us to compare asset value paths over time for the different leverage policies and, in turn, show what they imply for computations of default probablities. To begin, Figure 1 illustrates the static model by plotting time t on the horizontal axis and asset value V on the vertical axis. The firm's initial asset value is denoted by $V(0)$. In this version, the default barrier does not change and hence V_B is constant forever. In addition, there is no upper boundary in the static version (or rather the upper barrier is infinitely large, i.e. $V_R = \infty$), so the firm's default probability satisfies the conventional single barrier solution. The firm only resides in one stage (stage 1), because the default barrier does not change over time. Moreover, if the firm does not default and its asset value grows over time, as in the data, leverage would tend to zero.

[Insert Figure 1 here.]

By contrast, the dynamic model evolves over time as the firm moves through different restrucutring stages. Figure 2 summarizes this case graphically. In stage 1, the firm begins at $V^1(0)$ and either reaches the lower barrier V_B^1, at which point the firm declares bankruptcy, or the firm reaches V_R^1, at which point the debt is recalled at par value P and the firm again chooses an optimal capital structure, which will always be the same optimal (target) leverage ratio, because the firm is scaled by factor γ (to be specified endogenously) at each refinancing point. The asset value at the beginning of stage 2 is $V^2(0) = V_R^1 = \gamma\, V^1(0)$. Similarly, the default barrier scales up from stage 1 to stage 2 by the scaling factor γ, that is, $V_B^2 = \gamma\, V_B^1$. This scaling process continues forever unless the firm defaults. In contrast to the static model, if the firm does not default and its asset value grows

over time, as in the data, leverage would remain within an optimal range of non-trivial values.

[Insert Figure 2 here.]

For our sample from 1951 to 2023, we examine how future debt evolves relative to current debt. Figure 3 shows how the average ratio of a firm's nominal debt, scaled by the first observation in the first year when the firm has leverage greater or equal to 5%. This ratio is tracked over the next ten consecutive years on a logarithmic scale for firms with non-missing data. The figure reveals a consistent and significant increase in debt ratios over time. While firms' asset values generally grow as well, this should not be surprising. However, without corresponding increases in nominal debt, a firm's financial leverage would naturally decline toward zero (as discussed in the static model). Despite this, much of the credit risk literature often assumes constant debt levels.

[Insert Figure 3 here.]

To summarize, the graphs reveal that the assumption of a constant default boundary is an unrealistic simplificaiton for firms that reoptimize their capital structures over time. However, analytical complexity of computing default probabilities for the dynamic case has heretofore hindered academics and practitioners to rely on more precise estimates. Against this backdrop, our paper makes three contributions. First, the next section derives a simple integral equation for the default probability over a finite time horizon of a company that makes coupon payments on its debt and infrequently returns to its leverage target by increasing its debt unless it defaults on its debt. Second, we examine the quantitive significance of our new solution in a calibrated example. Third, the subsequent section takes the equation to the data to exaime its empirical relevance, which, for example, unconvers novel 'level' and 'slope' effects in the term structure of default probabilities.

3 Default Probabilities

This section presents our main result. First, we revisit the conventional default probability formula for a static model of capital structure (Black-Cox formula) and then characterize the default probability for the dynamic model of capital structure. We assume here that the default (and restructuring) boundaries are given.

3.1 Static Case Without Restructuring

We start with the base case in which the firm has a static debt policy and hence only an option to default on its debt, which it may find optimal to exercise in a low asset value state. Let us first recall the Merton (1974) model, in which default cannot occur before the zero-coupon bond matures at time T. The default barrier is denoted by V_B. It is straightforward to show that the default probability under the physical measure $\mathbb{P}$ at time $t = 0$ is given by

$$DP_M(T) \;:=\; \mathbb{P}(V(T) \leq V_B) = \Phi\left(d\right) \tag{1}$$

for $V(0) > V_B > 0$, where $\Phi(\cdot)$ is the standard normal distribution function and d is the "distance to default"

$$d = \frac{\mathbb{E}\left[\log(V(T))\right] - \log(V_B)}{\sigma\sqrt{T}} = \frac{\log(V_B/V(0)) - (\mu - \frac{1}{2}\sigma^2)T}{\sigma\sqrt{T}} \tag{2}$$

where $\mathbb{E}$ is the expectation under $\mathbb{P}$. To derive (1) one can simply transform the event of default in terms of the standard normal variable.

Now we assume that the default can happen before T, in particular, when the asset value process V reaches the constant level V_B from above. This can be the case if there are safety covenants or it is optimal for equity holders to do so. Let us define the default time T_B as the first time the process V hits the level V_B

$$T_B := \inf\{t > 0 : V(t) \leq V_B\} \tag{3}$$

and the cumulative default probability in the base case is defined as

$$DP_{BC}(T) := \mathbb{P}(T_B \leq T) = \mathbb{P}\left(\min_{0\leq t\leq T} V(t) \leq V_B\right) \tag{4}$$

for a T-year horizon under the physical measure where we notice that the default event is equivalent to the event that the minimum of V on $[0, T]$ is smaller or equal than V_B. Black and Cox (1976) show the cumulative default probability under the physical measure $\mathbb{P}$ at time $t = 0$ is given by

$$DP_{BC}(T) \;=\; \Phi\left(d\right) \;+\; \left(\frac{V(0)}{V_B}\right)^{1-2\mu/\sigma^2} \Phi(\hat{d}) \tag{5}$$

for $V(0) > V_B > 0$ where

$$\hat{d} = \frac{\log(V_B/V(0)) + (\mu - \frac{1}{2}\sigma^2)T}{\sigma\sqrt{T}}. \tag{6}$$

Notice that the first term in (5) corresponds to Merton's probability (1) for one-time default at time $t = T$ and the second term takes into the account the possibility of early default at times time $0 \leq t < T$.[4] To obtain the base case formula (5), the well-known results on first-passage time problems (or distribution of running maximum/minimum) for Brownian motion with drift can be employed (see e.g. Harrison (1985)).

3.2 Dynamic Case With Restructuring

We present now the main result of this paper allowing for debt dynamics. In addition to the option to default on its debt, which the firm may find optimal to exercise in a low asset value state, the firm also possess a refinancing right that may be optimal to trigger when asset values increase sufficiently. In the dynamic case, the default boundary is not anymore constant over time and, in fact, the evolution of the default boundary is contingent on a particular sample path of the asset value process in (see Figure 2). Thus, a company's cumulative default probability depends on the distribution of possible realizations of changes in default boundaries over time, which in turn, depend on the distribution of the asset value process.

To derive the probability of default up to some time T, we employ the scaling feature of the lognormal distribution that allows for a stationary leverage target (refinancing) policy, and certain results on the double-barrier passage time distributions (see Lin (1998) on the pricing of double-barrier options). We then invoke an induction argument and obtain an integral equation for a company's cumulative default probability.

Let us consider the initial default level $V_B(0) = V_B < V(0)$. The capital structure is leveraged up for the first time when V reaches $V_R > V_B$. We suppose that the leverage ratio becomes the same as at $t = 0$. For this, we denote $\gamma = V_R/V(0)$. Let us then define the sequence of stopping times

$$T_{R,n} = \inf\{t > T_{R,n-1} : V(t) = V_R \cdot \gamma^{n-1}\} \tag{7}$$

for stage $n \geq 1$ with $T_{R,0} = 0$. Time $T_{R,n}$ represents the end of stage n for $n \geq 1$, i.e., when the

[4]Even though Black and Cox (1976) assume a boundary that deterministically increases over time (e.g., due to a covenant), academics and practitioners typically use a constant boundary given by the firm's amount of book debt.

company switches back to its optimal (target) leverage ratio. We then define the default boundary (contingent on the realization of V) as

$$V_B(t) = \sum_{n=1}^{\infty} V_B \gamma^{n-1} 1_{\{T_{R,n-1} \leq t < T_{R,n}\}} \tag{8}$$

for $t > 0$ where 1_A is an indicator function

$$1_A = \begin{cases} 1 & \text{for} \quad \omega \in A \\ 0 & \text{for} \quad \omega \notin A \end{cases} \tag{9}$$

of some event $A \in \mathcal{F}$. We note that for fixed t only one indicator will be distinct from zero and hence we pick up the corresponding number n (contingent on path of X) of current stage. The default time is then given by

$$T_B = \inf\{t > 0 : V(t) = V_B(t)\} \tag{10}$$

which differs from (3) in that $V_B(t)$ depends on time t. Given these definitions, we can express the cumulative default probability over a fixed time horizon $[0, T]$ for the dynamic case (DC)

$$DP_{DC}(T) := \mathbb{P}(T_B \leq T) \tag{11}$$

where $T > 0$. The main difficulty here is that the default boundary is not constant over time and, in fact, stochastic. To tackle this problem, let us adopt the following definition:

Definition 1. *For the dynamic model's default probability, there are three mutually exclusive events:*

1. $A_1(T) = \{\omega \in \Omega : T_{R,1}(\omega) < \min(T, T_B(\omega))\}$, *which is that the first hitting time of* V_R *precedes the default probability's horizon* T *and the bankruptcy time* T_B*;*
2. $A_2(T) = \{\omega \in \Omega : T_B(\omega) < \min(T, T_{R,1}(\omega))\}$, *which is that the bankruptcy time* T_B *precedes the default probability's horizon* T *and the first restructuring time* $T_{R,1}$*;*
3. $A_3(T) = \{\omega \in \Omega : T < \min(T_{R,1}(\omega), T_B(\omega))\}$, *which is that the time* T *occurs before* V *reaches* V_R *or* V_B*.*

We define the probabilities of corresponding events as $\mathbb{P}(A_1(T))$, $\mathbb{P}(A_2(T))$, $\mathbb{P}(A_3(T))$. We now summarize our main result for computing default probability in the dynamic case.

Proposition 1. *The default probability $DP_{DC}(T)$ solves the linear Volterra integral equation*

$$DP_{DC}(T) = \mathbb{P}(A_2(T)) + \int_0^T g^R(t) DP_{DC}(T-t)\, dt \tag{12}$$

for $T > 0$ with the initial condition $DP_{DC}(0) = 0$ where

$$\begin{aligned}\mathbb{P}(A_2(T)) = &\left(\frac{V_B}{V(0)}\right)^{\mu/\sigma^2 - 1/2} \\ &\times \left\{ \sum_{n=0}^{\infty} \left[\mathrm{e}^{-a_n(\mu/\sigma - \sigma/2)} N\left(\frac{(\mu/\sigma - \sigma/2)\, T - a_n}{\sqrt{T}} \right) \right.\right. \\ &\qquad \left. + \mathrm{e}^{a_n(\mu/\sigma - \sigma/2)} N\left(-\frac{(\mu/\sigma - \sigma/2)\, T + a_n}{\sqrt{T}} \right) \right] \\ &\quad - \sum_{n=-\infty}^{-1} \left[\mathrm{e}^{a_n(\mu/\sigma - \sigma/2)} N\left(\frac{(\mu/\sigma - \sigma/2)\, T + a_n}{\sqrt{T}} \right) \right. \\ &\qquad \left.\left. + \mathrm{e}^{-a_n(\mu/\sigma - \sigma/2)} N\left(-\frac{(\mu/\sigma - \sigma/2)\, T - a_n}{\sqrt{T}} \right) \right] \right\}\end{aligned} \tag{13}$$

$$g^R(t) = \left(\frac{V_R}{V(0)}\right)^{\mu/\sigma^2 - 1/2} \exp\left\{ -\frac{1}{2} (\mu/\sigma - \sigma/2)^2\, t \right\} \sum_{n=-\infty}^{\infty} f\left(t; b_n\right) \tag{14}$$

$$f(t;a) = \frac{a}{\sqrt{2\pi t^3}} \mathrm{e}^{-a^2/2t}, \quad t > 0, \quad a > 0 \tag{15}$$

$$a_n = \frac{1}{\sigma} \log \frac{(V_R)^{2n} V(0)}{(V_B)^{2n+1}}, \quad n \in \mathbb{Z} \tag{16}$$

$$b_n = \frac{1}{\sigma} \log \frac{(V_R)^{2n+1}}{(V_B)^{2n} V(0)}, \quad n \in \mathbb{Z} \tag{17}$$

and $N(\cdot)$ is cdf of the standard normal distribution $\mathcal{N}(0,1)$.

Proof. As the sets $A_1(T), A_2(T)$ and $A_3(T)$ are mutually exclusive and $\Omega = A_1(T) \cup A_2(T) \cup A_3(T)$, we use the formula of total probability to obtain

$$\begin{aligned}\mathbb{P}(T_B \le T)) &= \sum_{i=1}^{3} \mathbb{P}(T_B \le T, A_i(T)) \\ &= \mathbb{P}(T_B \le T, A_1(T)) + \mathbb{P}(A_2(T)) \mathbb{P}(T_B \le T | A_2(T)) + \mathbb{P}(A_3(T)) \mathbb{P}(T_B \le T | A_3(T)) \\ &= \mathbb{P}(T_B \le T, A_1(T)) + \mathbb{P}(A_2(T))\end{aligned} \tag{18}$$

where we use the facts that $\mathbb{P}(T_B \le T | A_2(T)) = 1$ and $\mathbb{P}(T_B \le T | A_3(T)) = 0$. Both statements are obvious as under the event $A_2(T)$ the default time occurs before T and under the event $A_3(T)$ the default time did not happen before T.

Now we need to calculate probabilities $\mathbb{P}(T_B \leq T, A_1(T))$ and $\mathbb{P}(A_2(T))$. As they contain double barrier passage times, unlike in the simple, single barrier case, there are no trivial expressions and one has to rely, for instance, on series representation expressions. To this end, we employ formula for $\mathbb{P}(A_2(T))$ derived Lin (1998) (see equations (28)–(29) in the paper) and provided in (36) above.

It remains now to calculate the probability $\mathbb{P}(T_B \leq T, A_1(T))$. For this, we condition on the random time $T_{R,1}$ of hitting V_R given that it happens before bankruptcy time T_B and obtain that

$$\mathbb{P}(T_B \leq T, A_1(T)) = \int_0^T g^R(t)\mathbb{P}(T_B \leq T | T_{R,1} = t)dt = \int_0^T g^R(t) DP_{DC}(T-t)dt \tag{19}$$

where $g^R(t)$ the conditional probability density of time $T_{R,1}$. Using again the results from Lin (1998), the expression for g^R is given in (14) above. Given the scaling property, the probability $\mathbb{P}(T_B \leq T | T_{R,1} = t)$ becomes simply the original probability function $DP_{DC}(T-t)$ but with shorter remaining time $T - t$. Plugging the expression (19) into (18), we get that

$$DP_{DC}(T) = \mathbb{P}(A_2(T)) + \int_0^T g^R(t) DP_{DC}(T-t)dt. \tag{20}$$

■

The intuition behind the result in equation (12) is the following. The default probability consists of two terms. The first term in (12) corresponds to the probability of default in stage 1. The second term represents the case when the default occurs in subsequent stages; in particular, conditional on the time $T_{R,1} = t$ of the first restructuring (given that it happens before T and default time T_B) we face the same problem as at time 0 (due to the scaling feature) but with shorter maturity $T - t$. This leads to an integral term in equation (12). As we discuss below, this integral equation can be easily solved numerically for the unknown function $DP_{DC}(\cdot)$.[5]

3.3 Numerical Scheme

The equations (12) and (20) are linear integral equations of Volterra type with initial condition $DP_{DC}(0) = 0$. This type of equation is well known in the integral equation theory from both

[5] We note that simple change of variables in the integral term allows us to rewrite (12) as

$$DP_{DC}(T) = \mathbb{P}(A_2(T)) + \int_0^T g^R(T-t)\, DP_{DC}(t)\, dt. \tag{21}$$

theoretical and numerical points of view. In the finance literature, Volterra type integral equations (though nonlinear) are used to determine the optimal exercise boundary for finite maturity American call/put options (see e.g. Carr, Jarrow, and Myneni (1992) for derivation and Chapter 8 in Detemple (2006) for a detailed description of numerical scheme). More precisely, the American option's exercise boundary (as the function of time t) is the solution to a nonlinear integral equation of Volterra type. In our case, the integral equation is simpler, because the kernel is linear in $DP_{DC}(\cdot)$.

As the equation (20) is more general, we show how to solve it numerically to calculate the default probability $DP_{DC}(T)$. The numerical scheme we use is straightforward: let us fix $T > 0$ and discretize interval $[0, T]$ with grid size $h = T/N$ for large N. Therefore we have the grid $0 = t_0 < t_1 < \ldots < t_N = T$. We approximate the integral term in (20) by the following quadrature scheme

$$\int_0^{t_j} \left(g^R(t) + (1-p_d)\, g^B(t)\right) DP_{DC}(T-t)dt \approx h \sum_{i=1}^{j} \left(g^R(t_i) + (1-p_d)\, g^B(t_i)\right) DP_{DC}(t_j - t_i) \quad (22)$$

for $j = 1, \ldots, N$. We then define recursively the sequence $\pi_j := DP_{DC}(t_j)$ according to (12)

$$\pi_j = \mathbb{P}(A_2(t_j)) + h \sum_{i=1}^{j} \left(g^R(t_i) + (1-p_d)\, g^B(t_i)\right) DP_{DC}(t_j - t_i) \quad (23)$$

for $j = 1, \ldots, N$ with initial condition $\pi_0 = 0$. We note that we use the time t_j instead of T in (12) as it holds for all $T > 0$.

At the end, we will obtain approximation π_N of $DP_{DC}(T)$ and, in fact, we have the convergence of π_N to the true probability $DP_{DC}(T)$ as N goes to $+\infty$. We also note that by the nature of algorithm above we recover along the way the whole term structure of default probabilities $\{DP_{DC}(t_i), 0 \leq i \leq N\}$. This numerical scheme is easy to implement and provides fast computations for $\{DP_{DC}(t_i), 0 \leq i \leq N\}$ as it requires only recursive calculations in equation (23).

3.4 Laplace Transform

In this section, we present an alternative way to solve the equations (12) and (20). We will apply Laplace transform techniques. Again as the equation (12) is the special case of (20), we will focus on the latter one.

Now let us recall that the Laplace transform of some function $f(T)$ is the function $\mathcal{L}[f](s)$, which is a unilateral transform defined by

$$F(s) := \mathcal{L}[f](s) = \int_0^\infty e^{-sT} f(T) dT \tag{24}$$

for complex numbers s and the inverse Laplace transform is given by

$$f(T) = \mathcal{L}^{-1}[F](T) = \frac{1}{2\pi i} \lim_{a\to\infty} \int_{\gamma-ia}^{\gamma+ia} e^{sT} F(s) ds. \tag{25}$$

We now apply it to both sides of (20)

$$\mathcal{L}[DP_{DC}](s) = p_d \mathcal{L}[\mathbb{P}(A_2)](s) + (\mathcal{L}[g^R](s) + (1-p_d)\mathcal{L}[g^B](s))\mathcal{L}[DP_{DC}](s) \tag{26}$$

where we use the fact that Laplace transform of the convolution is the product of Laplace transforms. We then have that

$$\mathcal{L}[DP_{DC}](s) = \frac{p_d \mathcal{L}[\mathbb{P}(A_2)](s)}{1 - \mathcal{L}[g^R](s) - (1-p_d)\mathcal{L}[g^B](s)}. \tag{27}$$

Using definitions of $\mathbb{P}(A_2(T)), g^R(T)$ and $g^B(T)$, we can easily derive corresponding Laplace transforms

$$\mathcal{L}[\mathbb{P}(A_2)](s) = \frac{1}{s}\left(\frac{V_B}{V(0)}\right)^{\mu/\sigma^2 - 1/2} \left(\sum_{n=0}^{\infty} e^{-a_n \sqrt{2s + (\mu/\sigma - \sigma/2)^2}} - \sum_{n=-\infty}^{-1} e^{a_n \sqrt{2s + (\mu/\sigma - \sigma/2)^2}} \right) \tag{28}$$

$$\mathcal{L}[g^R](s) = \left(\frac{V_R}{V(0)}\right)^{\mu/\sigma^2 - 1/2} \sum_{n=-\infty}^{\infty} \frac{b_n e^{-\sqrt{2s((\mu/\sigma - \sigma/2)^2 + b_n^2)}}}{\sqrt{(\mu/\sigma - \sigma/2)^2 + b_n^2}} \tag{29}$$

$$\mathcal{L}[g^B](s) = \left(\frac{V_B}{V(0)}\right)^{\mu/\sigma^2 - 1/2} \sum_{n=-\infty}^{\infty} \frac{a_n e^{-\sqrt{2s((\mu/\sigma - \sigma/2)^2 + a_n^2)}}}{\sqrt{(\mu/\sigma - \sigma/2)^2 + a_n^2}}. \tag{30}$$

Finally, we compute $DP_{DC}(T)$ by applying standard numerical inversion methods to the equation (27)

$$DP_{DC}(T) = \mathcal{L}^{-1}\left[\frac{p_2 \mathcal{L}[\mathbb{P}(A_2)]}{1 - \mathcal{L}[g^R] - (1-p_d)\mathcal{L}[g^B]}\right](T) \tag{31}$$

for $T > 0$, where the inverse Laplace transform was defined in (25).

To summarize, we can calculate $DP_{DC}(T)$ by applying numerical inverse Laplace transform to the known functions and without solving the integral equation (20).

3.5 Calibrated Example

In this section, we rely on standard solutions of two versions of commonly used capital structure models (i.e., static and dynamic). Given reasonable parameter values, we only use these different model outputs of an otherwise identical baseline firm to consider the quantitative implications of allowing for debt restructuring for the term structure of default probabilites.[6]

The numerical results are based on a basic parameterization of the dynamic and static models to study commonalities and differences quantitatively as they apply to a company's default probability. The baseline parameters in Table 1 assume realistic values that are consistent with earlier studies, such as Huang and Huang (2012) or Feldhütter and Schaefer (2018). We note that we use the risk-neutral drift $\hat{\mu}$ to solve the capital structure problems and the physical drift μ for calculating the default probabilities. Finally, we normalize the initial unlevered asset value at $t = 0$ to $V_0 = 1$.

[Insert Table 1 here.]

For this baseline environment, Table 2 provides leverage policy values of the static and dynamic capital structure model solutions (details available upon request). In particular, it displays coupon rate (c), restructuring barrier (V_R), default barrier (V_B), and market leverage (D/F) for the static model in Panel A, and the dynamic model with firm value-maximizing refinancing in Panel B.

[Insert Table 2 here.]

It is well known that the option to restructure debt in the future (financial flexibility) lowers the firm's initially optimal leverage ratio substantially (see, e.g., Goldstein, Ju, and Leland (2001)). For example, leverage drops from 44% to 37% when moving from Panel A to Panel B in Table 2. However, it is perhaps less well-known that financial flexibility also reduces the endogenous (or equity value-maximizing) default barrier, not only because of lower leverage but also because of higher equity value attributable to refinancing option value. The default barrier declines from 0.24 to 0.20 when moving from Panel A to Panel B in Table 2. Panel B reports results for the case

[6] We only rely on dyanmic capital structure models to 'discipline' inputs for default barriers for default probabilities and note that 'model-free' leverage policy values could alternatively be taken from the empirical data of Section 4.

when the debt dynamics (i.e., V_R) are set once and for all at time 0 to maximize initial firm value, $F(V_0)$, i.e., first-best refinancing.

Figure 4 displays the results for the dynamic model and the static model using the correct default probability formulas. The dotted black line plots the static model's default probability term structure using the single-barrier solution from Section 3.1 (DP_{BC}). The solid blue line plots the dynamic model's default probability term structure using our new formula from Section 3.2 (DP_{DC}).

[Insert Figure 4 here.]

For the set of plausible input parameter values in Table 1 and the horizons up to 25 years, the default probabilities for the dynamic model are lower than the default probabilities from the static model (i.e., a 'level' effect). The reason is that the effect of initially lower leverage on default probability dominates the effect of eventually higher leverage (in case of refinancing) on default probability. Put another way, the option to issue more debt in the future, which our new solution explicitly recognizes, attenuates but does not overturn an initially lower default probability due to initially lower leverage at time 0 when upward restructuring options are available too.

Interestingly, for horizons longer than 25 years, the default probability for the dynamic model is larger than the default probability for the static case. Hence, Figure 4 reveals that the curves for the different default probability formulas can cross. This is intuitive in that our new solution takes into account the possibility of positive jumps in the default threshold at optimal restructuring times. If the asset value quickly rises so that the default threshold $V_B(t)$ jumps up sooner and becomes higher than the default level for the static model.

In another set of numerical simulations, we aim at isolating the effect of future refinancing on default probability. For this, we plug the dynamic model's default threshold $V_B = 0.20$ in Panel B of Table 2) into both DP_{DC} and DP_{BC}. Figure 5 depicts corresponding default probabilities and reveals that the term structure is steeper for the dynamic case (i.e., a 'slope' effect). As expected, we see that the default probability is higher when accounting for debt dynamics. Therefore, issuing more debt in the future introduces an underestimation bias in conventional (Black-Cox) default probability predictions. More importantly, however, Figure 5 isolates the effect of future refinancing

on default probability by comparing directly DP_{BC} to DP_{DC} for the same default barrier.

[Insert Figure 5 here.]

4 Empirical Results

In this section we use a panel data set of U.S. firms for the period 1951–2023 to provide a large-scale examination of our default probability formula's ability to capture the term structure of default rates and compare its implications with those from the Black-Cox model.

4.1 Data

In our empirical analysis, we use firm-level variables (for example, leverage and equity volatility) along with aggregate historical default rates and risk-free rates. We focus on the U.S. market, and our main data sources are Compustat for firm fundamentals, CRSP for stock returns and market capitalization, Standard & Poor's for entity credit ratings, Moody's for historical default rates, and the Federal Reserve Economic Data (FRED) database for Treasury yields.

The data sources are well known and used in a large number of studies. Below we provide a brief description of each.

Firm variables

For a given firm and calendar year, we obtain interest payments (INTPN), dividend payments (DVT), net stock repurchases (PRSTKC), debt in current liabilities (DLC), total long-term debt (DLTT) as well as industry classification from the CRSP/Compustat Merged Database. We assign annual firm fundamentals to the calendar with the most overlap (i.e., fiscal years ending in January to May are assigned to the prior calendar year) and use the last annual filing of a firm in a calendar year. We employ historical 4-digit standard industry classification codes (SICH) where available and otherwise current industry codes (SIC). The sample is limited to industrial firms and thus excludes utilities (SIC codes 4900–5000) and financials (SIC codes 6000–6999). The nominal amount of debt is calculated as the sum of debt in current liabilities and total long-term debt.

We obtain firm-level entity credit ratings for U.S. firms from Standard & Poor's. Ratings

are long-term issuer credit ratings (RatingTypeCode = "STDLONG" and OrgDebtTypeCode = "ICR"). We aggregate the available 33 rating levels into 7 broader rating categories, i.e., A (A, A+, +/A–1, A–, A/A, A/A–1), AA (AA, AA+, AA+/A–1+, AA–, AA–/A–1+), AAA (AAA, AAA/A–1+), B (B, B+, B+/B, B–), BB (BB, BB+, BB–), BBB (BBB, BBB+, BBB+/A–2, BBB-, BBB–/A–3, BBB/A–2), and C (C, CC, CCC, CCC+, CCC–). For each firm and rating date, we use the last available rating and carry it forward until the next rating update.

To calculate the financial leverage ratio of firm j at time t, we first compute the quasi-leverage ratio at time t as $L^j_{q,t}$=(nominal amount of debt)/(market value of equity + nominal amount of debt), where the market value of equity is calculated as the number of shares outstanding (SHROUT) times the (absolute value of the) closing share price at the fiscal year end date (PRC), summed across all common stocks of an issuer (share codes 10 and 11) traded on NYSE, Nasdaq and Amex (exchange codes 1, 2, and 3). Due to limited data on market values of debt, this is the measure of leverage commonly used in the literature, but theoretically it is correct to use the market leverage ratio, $L^j_{m,t}$=(nominal amount of debt)/(market value of equity + market value of debt) (see, for example, Merton (1974)). Bretscher, Feldhütter, Kane, and Schmid (2021) (BFKS) show that there are significant differences between quasi-leverage and market leverage. Given that we do not have complete data on market values of debt (we have corporate bond data but do not have market values for bank debt), we use BFKS's suggested approximation and calculate market-leverage as $L^j_{m,t} = 0.871 \times L^j_{q,t} + 0.311 \times (L^j_{q,t})^2$.

Equity volatility $\sigma^j_{E,t}$ is computed using daily stock returns (RET) from CRSP for the period between two fiscal year-end dates. We limit observations to common stock (share codes 10 and 11) traded on NYSE, Nasdaq and Amex (exchange codes 1, 2, and 3). For firms with several share classes, we use prior day market capitalization (calculated as the product of the absolute value of share price (PRC) and shares outstanding (SHROUT)) of each share class as weights to obtain a single daily return series for the issuer. The calculation of equity volatility requires at least 180 observations during the fiscal year; it is annualized by multiplying with the square root of 255.

We use the approximation in BFKS and calculate asset volatility $\sigma^j_{A,t}$ at time t as $\sigma^j_{A,t} = [1 - 1.129 \times L^j_{q,t} + 0.354 \times (L^j_{q,t})^2]\sigma^j_{E,t}$. For each firm, we calculate a constant asset volatility

parameter by computing the average asset volatility for the years the firm is in the sample.

The payout rate is the total outflow to stakeholders divided by firm value. This is computed as the sum of the previous year's interest payments, dividend payments, and net stock repurchases divided by the sum of market value of equity and book value of debt (as implied by $L^j_{m,t}$). The payout ratio is winsorized at 0.13 as in Feldhütter and Schaefer (2018) and lagged one year.

For a given firm and year, we use the leverage ratio, asset volatility, and rating at the end of the fiscal year, as well as the payout ratio at the end of the prior fiscal year. We restrict our attention to firm-years with available credit rating and positive values for leverage, equity volatility, prior-year payout ratio as well as (constant) asset volatility. We winsorize the left tail of leverage and asset volatility at 0.01. The number of firm-year observations for which we can calculate all firm values is 29,495, and the number of firms is 2,234. Firm summary statistics are in Table 3.

[Insert Table 3 here.]

Default data

We use historical default rates for the period 1920–2017 reported for horizons 1, ..., 20 years and for different ratings by Moody's (2023).

Riskfree Rate

We use the market yield on U.S. Treasury securities at 10-year constant maturity (not seasonally-adjusted) quoted on an investment basis (GS10) from the FRED database as risk-free rate. We use the value for the month of the fiscal year-end date. The swap rate is commonly used as risk-free rate, but we do not have swap rates in the first years.

4.2 Estimation of refinancing parameter

We estimate the default and refinancing parameters of the dynamic model and the Black-Cox model by matching model-implied default rates to historical ones. We do so by using the approach in Feldhütter and Schaefer (2018). The default probability in the Black-Cox model is given in equation (5), while the default probability in the dynamic model is given in equation (20).

In the Black-Cox model there is the lower default boundary V_B as the single parameter to

estimate. In the standard Merton model, the default boundary is given as the nominal amount of outstanding debt D. However, Davydenko (2013) shows that firms typically default when firm value is below the face value of debt and we therefore follow Feldhütter and Schaefer (2018) and estimate the fraction d of the nominal amount of debt at which the firm defaults when firm value reaches this point. That is, the firm defaults when firm value hits $d \times D$ and we estimate d such that the model gives the best fit to historical default rates.

In the dynamic model there is one additional parameter compared to the Black-Cox model: the upper refinancing boundary V_R. In the estimation, we make the simplifying assumption that the firm has just refinanced such that the ratio between the upper refinancing boundary and current firm value, $\frac{V_R}{V_t}$, is the same for all t. In this case we rewrite the upper default boundary as $V_R = u \times V_t$ and u has the intuitive interpretation that $u - 1$ is the percentage increase of current firm value at which the firm refinances.

For each default probability model, we estimate the parameters Θ (where $\Theta = d$ in the Black-Cox model, and $\Theta = (d, u)$ in the model with restructuring) separately for different rating categories. While the parameters in theory should be the same for all ratings, we find significant differences and we therefore allow them to be different across ratings to shed light on the cross-sectional heterogeneity of parameters across different levels of credit risk. For a given Θ we compute average model default probabilities for a given rating a in a manner similar to the way in which Moody's calculates historical default rates. More specifically, in each year we find all firms for which we have data and that have rating a, and for those firms we calculate the term structure of default probabilities, i.e. default probabilities for horizons of 1, 2,..., 20 years. We then calculate the average term structure of default probabilities for each year 1951, ... , 2023 and, finally, we compute the average term structure across years. This procedure leaves us with the average model-implied default probabilities $\overline{\pi}^P_{a1}(\Theta), \overline{\pi}^P_{a2}(\Theta), ..., \overline{\pi}^P_{a20}(\Theta)$, where $t = 1, ..., 20$ is the horizon in years.

We denote by $\hat{\pi}^P_{at}$ the corresponding historical default frequency. We find the parameters Θ that minimize the sum of absolute differences between the annualized historical and model-implied

default rates by solving

$$\min_{\{\Theta\}} \sum_{t=1}^{20} \frac{1}{t} \left| \overline{\pi}_{at}^{P}(\Theta) - \hat{\pi}_{at}^{P} \right|. \tag{32}$$

separately for ratings $a = AAA, AA, A, BBB, BB, B$, and C.

To calculate the drift in firm value in for firm j in year t, μ_{jt}, we assume a constant asset Sharpe ratio θ, and so $\mu_{jt} = \theta\sigma_A^j + r_t^T - \delta_{jt}$, where σ_A^j is the (constant) asset volatility of firm j, δ_{jt} is the payout rate for firm j in year t, and r_t^{10} is the 10-year riskfree rate in year t. As is common in the literature we use a Sharpe ratio of 0.22.

4.3 Results

The estimated parameters are reporeted in Table 4 along with the sum of weighted absolute errors (SWAE) that are minimized in (32). Across ratings and models, the average default boundary is between 0.77-0.84 times the face of debt and thus of similar magnitude as the estimate of 0.89 in Feldhütter and Schaefer (2018). For a given model, there is some variation of the default boundary estimate across individual rating categories, but it is unclear if the differences are statistically significant as Feldhütter and Schaefer (2018) show that there is significant statistical uncertainty when estimating the default boundary, particularly when using only investment grade default rates.

[Insert Table 4 here.]

In the model with restructuring, the parameter u determining when the firm upward restructures is on average estimated to be 2.02, and it is typically larger than 1 across ratings. Thus, firms are estimated to take on more debt on a frequent basis. The improvement on fit when allowing for restructuring is dramatic: on average SWAEs are more than thirteen times higher in the Black-Cox model. Figure 6 (and Table 5) shows that the slope of the term structure is too low in the Black-Cox model relative to the actual slope, and since the effect of upward restructuring is to increase the slope, it is estimated to be insignificant.

[Insert Figure 6 and Table 5 here.]

5 Conclusion

This paper studies how leverage targeting affects the measurement of default probabilities over economically relevant horizons. Structural models of credit risk are widely used to infer default probabilities from firm value dynamics, yet their practical implementations typically rely on a simplifying "passive debt" assumption under which the default boundary remains constant forever. We relax this assumption that implies a constant default boundary and develop a tractable structural framework that incorporates infrequent refinancing and leverage targeting into the measurement of default probabilities. In the model, default occurs when a firm's asset value falls to a lower boundary, while refinancing occurs when asset value rises to an upper boundary, increasing outstanding debt, and thereby shifting the effective default boundary upward. This simple mechanism captures the empirically observed tendency of firms to return to target leverage ratios whenever their asset values have evolved sufficiently, which in turn implies that default boundaries are not constant but evolve endogenously over time. The resulting framework for default probability modeling preserves the transparency and computational feasibility that have made structural models useful in practice while incorporating a basic but overlooked property of the financing behavior of companies.

The paper makes three contributions. First, we analytically characterize the cumulative default probabilities when firms can refinance and adjust leverage, showing that default probabilities can be expressed through a Volterra integral equation that generalizes the Black–Cox model. Second, we demonstrate quantitatively that the prospect of future refinancing steepens the term structure of default probabilities by raising future default boundaries for surviving firms, implying that constant-boundary models systematically understate long-horizon default risk. Third, using U.S. firm data from 1951–2023, we show empirically that refinancing-adjusted default probabilities match both the level and slope of realized default rates substantially better than the conventional model.

Beyond its empirical and practical importance, this paper's analysis helps bridge two strands of the literature that have largely evolved separately. Dynamic capital structure models emphasize firms' endogenous financing decisions, but are often difficult to implement for measuring default probabilities over finite horizons. In contrast, traditional structural default models offer analytical

tractability, but typically abstract from leverage adjustment. By incorporating compelling debt dynamics into a tractable default probability setting, our work connects two important literatures and provides analytical results that are both economically grounded and empirically implementable.

There are several directions for future research that emerge from our paper's analysis. An important avenue is to enrich the refinancing mechanism by allowing for debt renegotiation, downward restructuring, or maturity structure choices. Another is to embed the framework in a broader equilibrium setting in which refinancing opportunities depend on fluctuations in credit market conditions, credit supply, and macroeconomic conditions. Moreover, it would be fruitful to examine the role of debt dynamics for corporate bond pricing, credit spreads, and credit derivatives (e.g., credit default swaps), where long-horizon default probabilities play a central role.

Taken together, the results of this paper suggest that modeling debt dynamics is essential to accurately measure default risk over longer horizons. By providing a tractable way to incorporate refinancing and leverage targeting into a credit risk model, our framework offers a step toward improving the measurement of default probabilities in empirical work and in practical applications of structural models to make them more useful.

References

Bhamra, Harjoat S, Lars-Alexander Kuehn, and Ilya A Strebulaev, 2010, The levered equity risk premium and credit spreads: A unified framework, *Review of Financial Studies* 23, 645–703.

Black, Fischer, and John Cox, 1976, Valuing corporate securities: Some effects of bond indenture provisions, *Journal of Finance* 31, 351–67.

Bretscher, Lorenzo, Peter Feldhütter, Andrew Kane, and Lukas Schmid, 2021, Marking to Market Corporate Debt, *Working Paper*.

Carr, Peter, Robert Jarrow, and Ravi Myneni, 1992, Alternative characterizations of american put options, *Mathematical Finance* 2, 87–106.

Chen, Hui, 2010, Macroeconomic conditions and the puzzles of credit spreads and capital structure, *Journal of Finance* 65, 2171–2212.

Collin-Dufresne, Pierre, and Robert S. Goldstein, 2001, Do credit spreads reflect stationary leverage ratios?, *Journal of Finance* 56, 1929–1957.

Davydenko, Sergei A., 2013, When do firms default? A Study of the Default Boundary, *Working paper*.

Detemple, Jerome, 2006, *American-Style Derivatives: Valuation and Computation* (Chapman and Hall/CRC).

Eom, Young Ho, Jean Helwege, and Jing-Zhi Huang, 2004, Structural models of corporate bond pricing: An empirical analysis, *Review of Financial Studies* 17, 499–544.

Feldhütter, Peter, and Stephen Schaefer, 2018, The myth of the credit spread puzzle, *Review of Financial Studies* 31, 2897–2942.

Fischer, Edwin O, Robert Heinkel, and Josef Zechner, 1989, Dynamic capital structure choice: Theory and tests, *Journal of Finance* 44, 19–40.

Goldstein, Robert, Nengjiu Ju, and Hayne Leland, 2001, An EBIT-based model of dynamic capital structure, *Journal of Business* 74, 483–512.

Hackbarth, Dirk, Jianjun Miao, and Erwan Morellec, 2006, Capital structure, credit risk, and macroeconomic conditions, *Journal of Financial Economics* 82, 519–550.

Harrison, Michael, 1985, *Brownian Motion and Stochastic Flow Systems* (Wiley, New York).

Huang, Jing-Zhi, and Ming Huang, 2012, How much of the corporate-treasury yield spread is due to credit risk?, *Review of Asset Pricing Studies* 2, 153–202.

Huang, Jing-Zhi, Yoshio Nozawa, and Zhan Shi, 2025, The global credit spread puzzle, *Journal of Finance* 80, 101–162.

Jeanblanc, Monique, Marc Yor, and Marc Chesney, 2006, *Mathematical Methods for Financial Markets* (Springer, Berlin).

Leland, Hayne, 1994, Corporate debt value, bond covenants, and optimal capital structure, *Journal of Finance* 49, 1213–1252.

Lin, X. Sheldon, 1998, Double barrier hitting time distributions with applications to exotic options, *Insurance: Mathematics and Economics,* 21, 45–58.

Merton, Robert, 1974, On the pricing of corporate debt: The risk structure of interest rates, *Journal of Finance* 29, 449–70.

Moody's, 2023, Annual Default Study: Corporate Default and Recovery Rates, 1920-2022, *Moody's Investors Service* pp. 1–60.

Pelsser, Antoon, 2000, Pricing double barrier options using Laplace transforms, *Finance and Stochastics* 4, 95–104.

Strebulaev, Ilya, 2007, Do tests of capital structure theory mean what they say?, *Journal of Finance* 62, 1747–1787.

Appendix. Detailed Derivation of $DP_{DC}(T)$ in Proposition 1

Setup and Notation

Let $(\Omega, \mathcal{F}, \{\mathcal{F}_t\}_{t\geq 0}, \mathbb{P})$ be a filtered probability space satisfying the usual conditions. Let $W = \{W_t, t \geq 0\}$ be a standard, one-dimensional $\{\mathcal{F}_t\}$-Brownian motion with $W_0 = 0$.

We consider the logarithmic asset process with drift μ and volatility $\sigma > 0$:

$$X_t = \log(V(0)) + \left(\mu - \frac{\sigma^2}{2}\right) t + \sigma W_t$$

Define two absorbing boundaries representing the lower and upper thresholds, respectively:

$$a = \log(V_B) \quad \text{and} \quad b = \log(V_R)$$

We assume $V_B < V(0) < V_R$.

For any target level $y \in \mathbb{R}$, define the first hitting time of y by the process as:

$$H_y = \inf\{t > 0 : X_t = y\}$$

Equation (13)

Let $\tau_B = H_a$ and $\tau_R = H_b$. The sub-probability density function $g^R(t)$ of the event that the process hits the upper barrier V_R at time t before ever hitting the lower barrier V_B, denoted as $\{\tau_R \in dt, \tau_R < \tau_B\}$, is given by:

$$g^R(t) = \left(\frac{V_R}{V(0)}\right)^{\mu/\sigma^2 - 1/2} \exp\left\{-\frac{1}{2}\left(\mu/\sigma - \sigma/2\right)^2 t\right\} \sum_{n=-\infty}^{\infty} f\left(t; b_n\right) \tag{33}$$

$$f(t; a) = \frac{a}{\sqrt{2\pi t^3}} \mathrm{e}^{-a^2/2t}, \quad t > 0, \quad a > 0 \tag{34}$$

$$b_n = \frac{1}{\sigma} \log \frac{(V_R)^{2n+1}}{(V_B)^{2n} V(0)}, \quad n \in \mathbb{Z} \tag{35}$$

Part 1 of Proof: The Driftless Baseline Measure $\mathbb{Q}$

We first define an equivalent martingale measure $\mathbb{Q}$ under which the drift is removed. Under $\mathbb{Q}$, the process is a purely volatility-scaled Brownian motion:

$$X_t = \log(V(0)) + \sigma W_t^{\mathbb{Q}}$$

We define the fundamental probability density function of a standard Brownian motion traversing an unrestricted, standardized distance z as the Lévy distribution $f(t;z)$ defined in Equation (34).

To find the hitting time density of the upper barrier prior to the lower barrier under $\mathbb{Q}$, we apply the principle of inclusion-exclusion via the Reflection Principle. We construct two alternating sequences of stopping times reflecting across the boundaries a and b.

The cumulative unfolded straight-line distances required to satisfy the absorbing boundary conditions are generated by an infinite sequence of reflections. The unscaled effective distances are:

$$d_n = (b - X_0) + 2n(b - a) = \log\left(\frac{V_R}{V(0)}\right) + 2n\log\left(\frac{V_R}{V_B}\right) \quad \text{for } n \in \mathbb{Z}$$

Because our process X_t is scaled by σ, we must standardize these distances to evaluate them using the standard density $f(t;\cdot)$. We define the standardized distances $b_n = d_n/\sigma$:

$$b_n = \frac{1}{\sigma}\left[\log\left(\frac{V_R}{V(0)}\right) + 2n\log\left(\frac{V_R}{V_B}\right)\right] = \frac{1}{\sigma}\log\frac{(V_R)^{2n+1}}{(V_B)^{2n}V(0)}$$

This explicitly yields Equation (35).

By summing the fundamental densities evaluated at these standardized alternating distances, the sub-probability density function under the driftless measure $\mathbb{Q}$ is exactly:

$$g^R_{\mathbb{Q}}(t) = \sum_{n=-\infty}^{\infty} f(t; b_n)$$

Part 2 of Proof: Application of Girsanov's Theorem

To find the true density $g^R(t)$ under the real-world measure $\mathbb{P}$, we apply Girsanov's Theorem. Let the drift of the process be $\nu = \mu - \frac{\sigma^2}{2}$. The Radon-Nikodym derivative for the change of measure evaluated at the stopping time $\tau_R = t$ is:

$$\left.\frac{d\mathbb{P}}{d\mathbb{Q}}\right|_{\tau_R = t} = \exp\left(\frac{\nu}{\sigma^2}(X_t - X_0) - \frac{\nu^2}{2\sigma^2}t\right)$$

Conditional on the process hitting the upper barrier at time t, the terminal position is strictly deterministic: $X_t - X_0 = b - X_0 = \log\left(\frac{V_R}{V(0)}\right)$.

We substitute this deterministic distance and the definition of ν into the Radon-Nikodym derivative. We first isolate the spatial weighting term:

$$\exp\left(\frac{\mu-\sigma^2/2}{\sigma^2}\log\left(\frac{V_R}{V(0)}\right)\right)=\exp\left(\left(\frac{\mu}{\sigma^2}-\frac{1}{2}\right)\log\left(\frac{V_R}{V(0)}\right)\right)=\left(\frac{V_R}{V(0)}\right)^{\mu/\sigma^2-1/2}$$

Next, we isolate the temporal weighting term:

$$\exp\left(-\frac{\nu^2}{2\sigma^2}t\right)=\exp\left(-\frac{(\mu-\sigma^2/2)^2}{2\sigma^2}t\right)=\exp\left(-\frac{1}{2}\left(\frac{\mu}{\sigma}-\frac{\sigma}{2}\right)^2 t\right)$$

The density under the physical measure $\mathbb{P}$ is the product of the driftless density $g^R_{\mathbb{Q}}(t)$ and the Radon-Nikodym derivative evaluated at the boundary:

$$g^R(t)=\left.\frac{d\mathbb{P}}{d\mathbb{Q}}\right|_{\tau_R=t} g^R_{\mathbb{Q}}(t)$$

Substituting our derived components yields:

$$g^R(t)=\left(\frac{V_R}{V(0)}\right)^{\mu/\sigma^2-1/2}\exp\left\{-\frac{1}{2}\left(\mu/\sigma-\sigma/2\right)^2 t\right\}\sum_{n=-\infty}^{\infty} f\left(t;b_n\right)$$

This establishes Equation (33) and concludes the proof. ■

Equation (14)

The probability $P(A_2(T))$ is given by the exact analytical formula:

$$\begin{aligned}P(A_2(T))=&\left(\frac{V_B}{V(0)}\right)^{\mu/\sigma^2-1/2}\\&\times\left\{\sum_{n=0}^{\infty}\left[\mathrm{e}^{-a_n(\mu/\sigma-\sigma/2)}N\left(\frac{(\mu/\sigma-\sigma/2)\,T-a_n}{\sqrt{T}}\right)\right.\right.\\&\qquad\left.+\mathrm{e}^{a_n(\mu/\sigma-\sigma/2)}N\left(-\frac{(\mu/\sigma-\sigma/2)\,T+a_n}{\sqrt{T}}\right)\right]\\&\quad-\sum_{n=-\infty}^{-1}\left[\mathrm{e}^{a_n(\mu/\sigma-\sigma/2)}N\left(\frac{(\mu/\sigma-\sigma/2)\,T+a_n}{\sqrt{T}}\right)\right.\\&\qquad\left.\left.+\mathrm{e}^{-a_n(\mu/\sigma-\sigma/2)}N\left(-\frac{(\mu/\sigma-\sigma/2)\,T-a_n}{\sqrt{T}}\right)\right]\right\}\end{aligned}\tag{36}$$

where $N(\cdot)$ is the standard normal cumulative distribution function, and the standardized distance parameter a_n is defined as:

$$a_n=\frac{1}{\sigma}\log\frac{(V_R)^{2n}V(0)}{(V_B)^{2n+1}},\quad n\in\mathbb{Z}\tag{37}$$

Part 1 of Proof: The Driftless Lower Boundary Hitting Density

We first establish the hitting time density of the lower barrier prior to the upper barrier under the driftless equivalent martingale measure $\mathbb{Q}$. By symmetry to the derivation of the upper boundary hitting density, we apply the inclusion-exclusion principle.

The paths valid for $P(A_2(T))$ are those that hit $a = \log(V_B)$ without first hitting $b = \log(V_R)$. The unfolded unscaled distances required to satisfy the absorbing boundaries are generated by infinite reflections. The positive standardized distances a_n are constructed by normalizing by the volatility σ, yielding Equation (37).

- For $n \geq 0$, a_n represents the strictly positive standardized distances of the valid paths initiating toward the lower boundary.
- For $n < 0$, let $n = -m$ where $m \geq 1$. The term a_{-m} evaluates to a strictly negative number. Its absolute value, $|a_{-m}| = -a_{-m}$, exactly corresponds to the positive standardized distances of the invalid contaminating paths initiating toward the upper boundary, which must be subtracted.

Using the fundamental standardized density $f(t;d) = \frac{d}{\sqrt{2\pi t^3}} \exp\left(-\frac{d^2}{2t}\right)$, the driftless density of hitting the lower boundary first is cleanly expressed as:

$$g^B_{\mathbb{Q}}(t) = \sum_{n=0}^{\infty} f(t;a_n) - \sum_{n=-\infty}^{-1} f(t;-a_n)$$

Part 2 of Proof: Girsanov's Theorem and Spatial Weighting

We revert to the physical measure $\mathbb{P}$ using Girsanov's Theorem. Let the standardized drift parameter be defined as $\hat{\nu} = \frac{\mu}{\sigma} - \frac{\sigma}{2}$. The Radon-Nikodym derivative evaluated at the deterministic spatial boundary $\tau_B = t$ introduces a fixed spatial weight and a time-dependent weight.

Because the process terminates exactly at V_B, the spatial weight factors out entirely from the summation:

$$\exp\left(\frac{\mu - \sigma^2/2}{\sigma^2} \log\left(\frac{V_B}{V(0)}\right)\right) = \left(\frac{V_B}{V(0)}\right)^{\mu/\sigma^2 - 1/2}$$

This establishes the leading factor in Equation (36). The full density under $\mathbb{P}$ inside the summation is thus weighted by the temporal decay $\exp\left(-\frac{\hat{\nu}^2 t}{2}\right)$.

Part 3: Time Integration

The cumulative probability $P(A_2(T))$ is the time integral of this drifted density from 0 to T. This requires evaluating integrals of the form:

$$I(d) = \int_0^T f(t;d) \exp\left(-\frac{\hat{\nu}^2 t}{2}\right) dt = \int_0^T \frac{d}{\sqrt{2\pi t^3}} \exp\left(-\frac{d^2 + \hat{\nu}^2 t^2}{2t}\right) dt$$

for any strictly positive distance $d > 0$. This is the standard integral of the Inverse Gaussian distribution, yielding the known closed-form identity:

$$I(d) = \mathrm{e}^{-d\hat{\nu}} N\left(\frac{\hat{\nu}T - d}{\sqrt{T}}\right) + \mathrm{e}^{d\hat{\nu}} N\left(-\frac{\hat{\nu}T + d}{\sqrt{T}}\right)$$

We apply this integration term-by-term to our infinite series:

- For the added paths ($n \geq 0$), the distance is strictly $d = a_n > 0$. Substituting a_n into the identity $I(d)$ explicitly generates the terms inside the first summation of Equation (36).
- For the subtracted paths ($n \leq -1$), the distance is strictly $d = -a_n > 0$. Substituting $-a_n$ into the identity $I(d)$ yields:

  $$I(-a_n) = \mathrm{e}^{-(-a_n)\hat{\nu}} N\left(\frac{\hat{\nu}T - (-a_n)}{\sqrt{T}}\right) + \mathrm{e}^{(-a_n)\hat{\nu}} N\left(-\frac{\hat{\nu}T + (-a_n)}{\sqrt{T}}\right)$$

  Simplifying the signs results exactly in:

  $$I(-a_n) = \mathrm{e}^{a_n\hat{\nu}} N\left(\frac{\hat{\nu}T + a_n}{\sqrt{T}}\right) + \mathrm{e}^{-a_n\hat{\nu}} N\left(-\frac{\hat{\nu}T - a_n}{\sqrt{T}}\right)$$

Applying the inclusion-exclusion subtraction strictly generates the negative sum in Equation (36). Recombining these integrated series with the factored spatial Girsanov weight completes the rigorous derivation of $P(A_2(T))$ and concludes the proof. ■

Figure 1. Asset Value Path and Default Barrier in Base Case of Static Capital Structure

The figure plots a hypothetical trajectory of firm value $V(t)$ and the default threshold V_B in the base case of static capital structure. Default happens when firm value drops to V_B at time T_B.

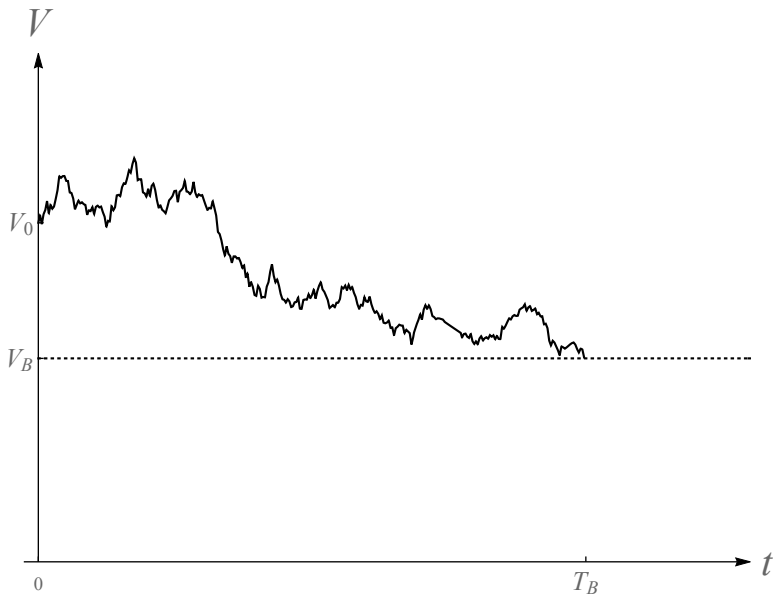


Figure 2. Asset Value Path and Barriers for Default and Restructuring in Case of Dynamic Capital Structure

The figure plots a hypothetical trajectory of firm value $V(t)$ and the evolution of the restructuring boundary V_R and default threshold V_B in the case of dynamic capital structure. When firm value increases to the restructuring boundary, the firm can issue additional debt, and the restructuring boundary and default threshold increase. Default happens when firm value drops to V_B at time T_B.

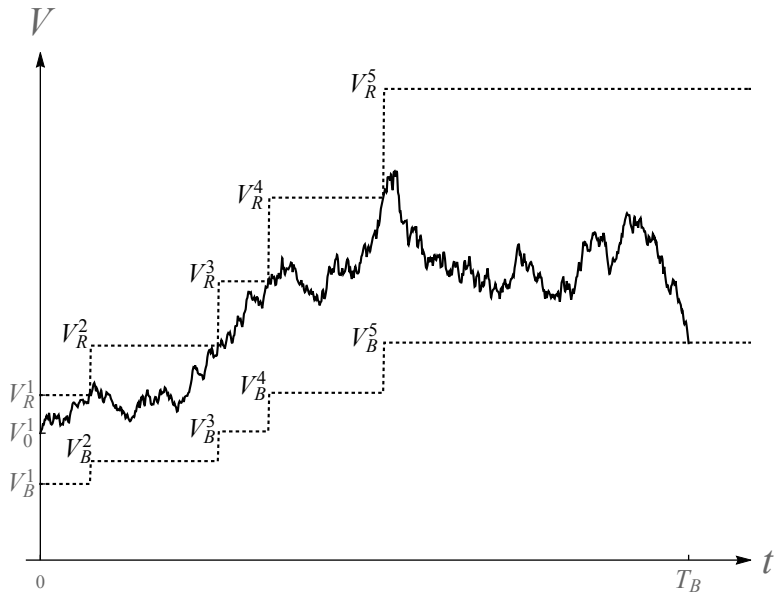


Figure 3. Future Debt Relative to Current Debt

The figure plots the average ratio of nominal debt of a firm scaled by the first observation in the first year where the firm has leverage greater or equal to 5% for our sample from 1951 to 2023. The graph plots the average nominal debt ratio for all firms with non-missing data for the first 10 consecutive years on a logarithmic scale.

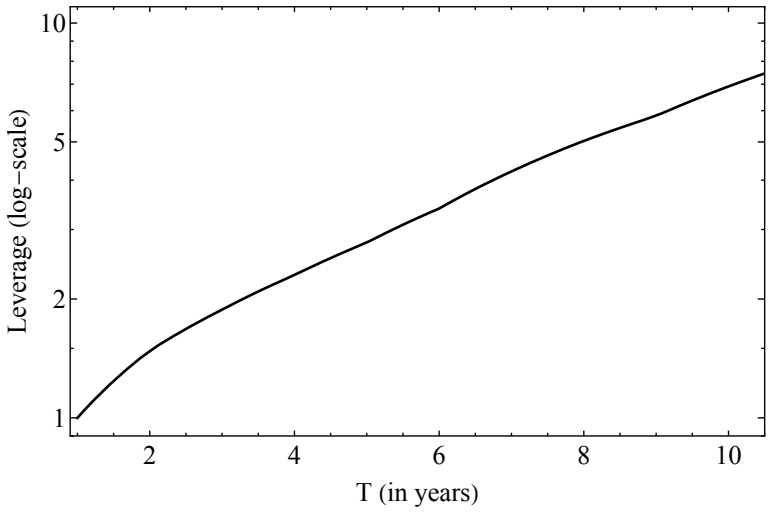


Figure 4. Term Structure of Default Probability

The figure plots constant-barrier default probability DP_{BC} for the model with static capital structure (black dashed line) and changing-barrier default probability DP_{DC} for the model with dynamic capital structure (blue solid line).

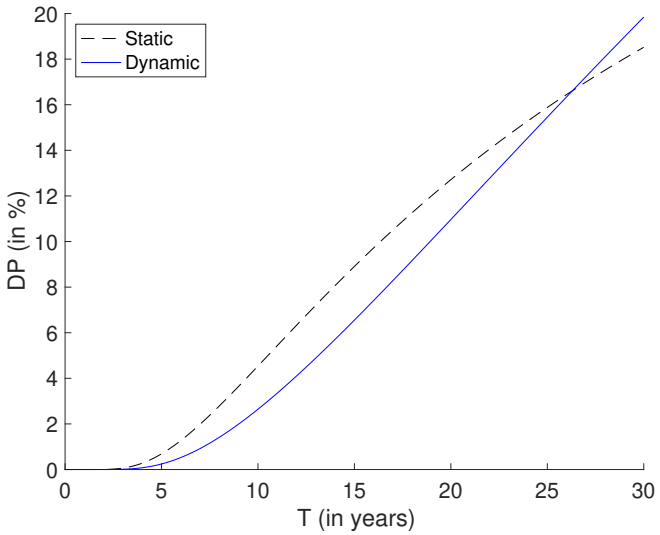


Figure 5. Effect of Refinancing on the Term Structure of Default Probability

The figure shows the constant-barrier default probability DP_{BC} (black dashed line) using the dynamic model's default barrier versus the changing-barrier default probability DP_{DC} (blue solid line), which isolates the effect of future refinancing on default probability.

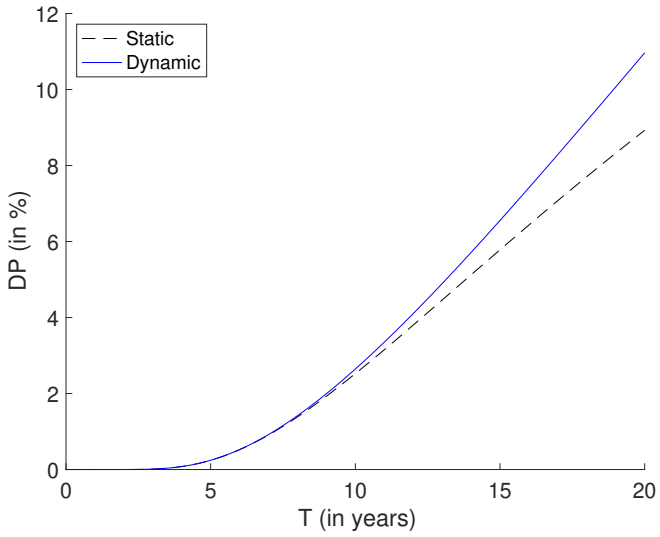


Figure 6. Average Cumulative Actual and Model-Implied Default Rates

The figure shows average cumulative actual and model-implied default rates by rating category for horizons of 1 to 20 years. In particular, for each rating category from AAA to C, it reports the average actual historical default rates from Moody's for the period 1920-2022 ('Actual'). In addition, it shows average model-implied default probabilities separately for the Black-Cox model (where the growth rate of debt is zero) ('Black-Cox Model') and the model allowing firms to issue more debt if leverage falls below a threshold and to restructure debt in case of default ('Restructuring Model'). Model-implied default probabilities are calculated for a sample of 29,495 firm-years over the period 1951-2023.

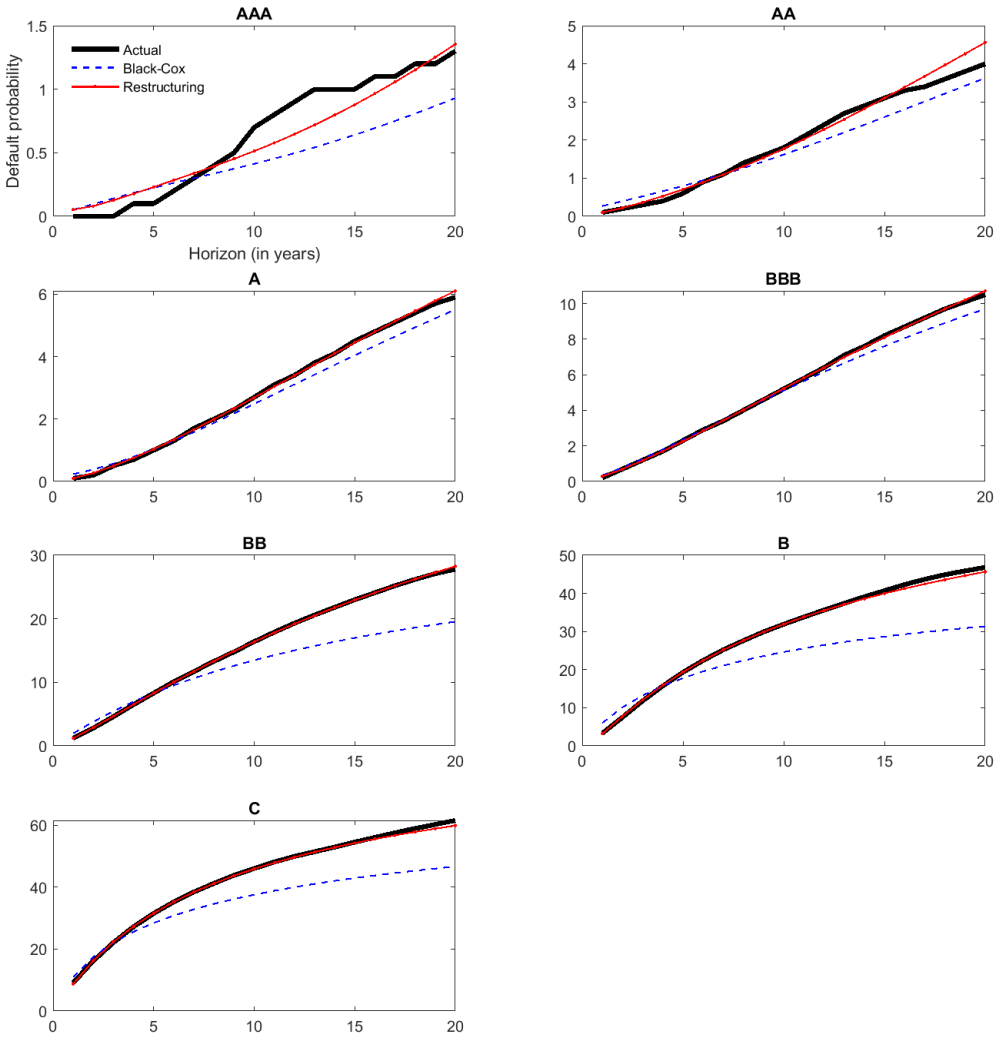


Table 1. Parameter Values

This table provides the parameter values used for the calibrated example in Section 3.5.

Quantity	Symbol	Value
Initial asset value	V_0	1
Growth rate of V (physical)	μ	0.05
Volatility of V	σ	0.25
Volatility of Λ	σ_Λ	0.64
Correlation of Λ and V	ρ	–0.25
Market price of risk	π	0.04
Risk-free interest rate	r	0.05
Growth rate of V (risk-neutral)	$\hat{\mu}$	0.01

Table 2. Leverage Policy Value

The table provides outputs of the static and dynamic capital structure model solutions. It displays the coupon rate (c), restructuring barrier (V_R), default barrier (V_B), and market leverage (D/F).

	Coupon Rate	V_R	V_B	*Leverage* (D/F)
Static Model (No Refinancing)	0.61	∞	0.24	44.4%
Dynamic Model	0.51	2.45	0.20	37.1%

Table 3. Summary Statistics of Firm Variables

The table shows summary statistics for the firm-level variables Market Leverage Ratio (Panel A), Equity Volatility (Panel B), Asset Volatility (Panel C), and Payout Ratio (Panel D). In particular, it shows the number of unique sample firms, the mean, 10th percentile, 25th percentile, median, 75th percentile, and 90th percentile for each variable. The summary statistics are reported by rating class as well as for all firms.

Credit Rating	Number of Firms	Mean	10th	25th	Median	75th	90th
Panel A: Market Leverage ratio							
AAA	38	0.12	0.02	0.04	0.07	0.16	0.29
AA	135	0.16	0.04	0.07	0.13	0.21	0.33
A	384	0.20	0.05	0.09	0.16	0.27	0.40
BBB	700	0.27	0.07	0.13	0.22	0.36	0.54
BB	1,169	0.36	0.09	0.17	0.30	0.51	0.73
B	1,217	0.53	0.12	0.27	0.49	0.77	0.99
C	272	0.57	0.04	0.20	0.58	0.93	1.09
All firms	2,234	0.34	0.06	0.13	0.26	0.48	0.75
Panel B: Equity volatility							
AAA	38	0.23	0.16	0.18	0.22	0.27	0.34
AA	135	0.27	0.17	0.21	0.25	0.31	0.38
A	384	0.30	0.19	0.22	0.27	0.34	0.44
BBB	700	0.34	0.20	0.25	0.31	0.40	0.51
BB	1,169	0.45	0.25	0.31	0.40	0.53	0.71
B	1,217	0.63	0.33	0.40	0.53	0.73	1.04
C	272	0.81	0.39	0.51	0.68	0.95	1.36
All firms	2,234	0.43	0.21	0.27	0.36	0.51	0.72
Panel C: Asset volatility							
AAA	38	0.20	0.17	0.17	0.20	0.22	0.23
AA	135	0.22	0.17	0.19	0.21	0.24	0.28
A	384	0.24	0.18	0.20	0.23	0.26	0.32
BBB	700	0.26	0.19	0.21	0.24	0.29	0.35
BB	1,169	0.30	0.20	0.24	0.28	0.35	0.43
B	1,217	0.34	0.21	0.25	0.31	0.41	0.51
C	272	0.37	0.22	0.27	0.35	0.44	0.57
All firms	2,234	0.28	0.19	0.22	0.26	0.32	0.43
Panel D: Payout ratio							
AAA	38	0.034	0.016	0.022	0.032	0.042	0.056
AA	135	0.034	0.012	0.020	0.030	0.042	0.058
A	384	0.038	0.010	0.020	0.032	0.049	0.072
BBB	700	0.040	0.009	0.018	0.032	0.053	0.082
BB	1,169	0.038	0.006	0.014	0.029	0.053	0.084
B	1,217	0.045	0.005	0.015	0.037	0.066	0.099
C	272	0.055	0.007	0.022	0.049	0.083	0.124
All firms	2,234	0.040	0.007	0.017	0.032	0.054	0.085

Table 4. Parameter Estimates and Model Fit

The table shows estimated model parameters and model fit for the Black-Cox model and the model with restructuring, estimated by rating category. For both models, we estimate, for each rating category, the parameters in the minimization $\min_{\{\Theta\}} \sum_{t=1}^{20} \frac{1}{t} \left| \overline{\pi}_{at}^{P}(\Theta) - \hat{\pi}_{at}^{P} \right|$, where $\overline{\pi}_{at}^{P}(\Theta)$ is the model-implied average default probability for rating a and year t and $\hat{\pi}_{at}^{P}$ is the corresponding historical default frequency. For the optimization, we put an upper bound of 1,000 on u. SWAE (Sum of Weighted Absolute Errors) is equal to $\sum_{t=1}^{20} \frac{1}{t} \left| \overline{\pi}_{at}^{P}(\Theta) - \hat{\pi}_{at}^{P} \right|$. In particular, for the Black-Cox model, the table shows the parameter d as well as the Sum of Weighted Absolute Errors ($SWAE_{BC}$). For the model with restructuring, it shows the estimates for parameters d and u, as well as the Sum of Weighted Absolute Errors ($SWAE_{RES}$). The last column shows the ratio of $SWAE_{BC}$ to $SWAE_{RES}$. The last row shows averages across rating categories.

	Black-Cox Model		Restructuring Model			Model Comparison
	$\hat{d}$	$SWAE_{BC}$	$\hat{d}$	$\hat{u}$	$SWAE_{RES}$	$\frac{SWAE_{BC}}{SWAE_{RES}}$
AAA	0.81	0.0051	0.74	1.13	0.0033	1.55
AA	1.10	0.0079	0.94	1.09	0.0024	3.29
A	0.91	0.0061	0.93	3.28	0.0026	2.35
BBB	0.80	0.0062	0.79	3.89	0.0022	2.80
BB	0.77	0.0658	0.70	1.70	0.0019	34.45
B	0.74	0.1584	0.63	1.29	0.0083	19.12
C	0.72	0.1541	0.68	1.77	0.0093	16.62
Average	0.84	0.0577	0.77	2.02	0.0043	13.47

Table 5. Average Cumulative Actual and Model-Implied Default Rates

The table shows average cumulative actual and model-implied default rates by rating category for horizons of 1 to 20 years. In particular, for each rating category from AAA to C, it reports the average actual historical default rates from Moody's for the period 1920-2022 ('Actual'). In addition, it shows average model-implied default probabilities separately for the Black-Cox model (where the growth rate of debt is zero) ('Black-Cox Model') and the a model allowing firms to issue more debt if leverage falls below a threshold and to restructure debt in case of default ('Restructuring Model'). Model-implied default probabilities are calculated for a sample of 29,495 firm-years over the period 1951-2023.

		Horizons (Years)														
		1	2	3	4	5	6	7	8	9	10	12	14	16	18	20
AAA	Actual Default Rates	0.00	0.00	0.00	0.00	0.00	0.00	0.00	0.00	0.01	0.01	0.01	0.01	0.01	0.01	0.01
	Black-Cox Model	0.00	0.00	0.00	0.00	0.00	0.00	0.00	0.00	0.00	0.00	0.00	0.01	0.01	0.01	0.01
	Restructuring Model	0.00	0.00	0.00	0.00	0.00	0.00	0.00	0.00	0.00	0.01	0.01	0.01	0.01	0.01	0.01
AA	Actual Default Rates	0.00	0.00	0.00	0.00	0.01	0.01	0.01	0.01	0.02	0.02	0.02	0.03	0.03	0.04	0.04
	Black-Cox Model	0.00	0.00	0.01	0.01	0.01	0.01	0.01	0.01	0.01	0.02	0.02	0.02	0.03	0.03	0.04
	Restructuring Model	0.00	0.00	0.00	0.01	0.01	0.01	0.01	0.01	0.02	0.02	0.02	0.03	0.03	0.04	0.05
A	Actual Default Rates	0.00	0.00	0.01	0.01	0.01	0.01	0.02	0.02	0.02	0.03	0.03	0.04	0.05	0.05	0.06
	Black-Cox Model	0.00	0.00	0.01	0.01	0.01	0.01	0.02	0.02	0.02	0.02	0.03	0.04	0.04	0.05	0.06
	Restructuring Model	0.00	0.00	0.00	0.01	0.01	0.01	0.02	0.02	0.02	0.03	0.03	0.04	0.05	0.05	0.06
BBB	Actual Default Rates	0.00	0.01	0.01	0.02	0.02	0.03	0.03	0.04	0.05	0.05	0.06	0.08	0.09	0.10	0.10
	Black-Cox Model	0.00	0.01	0.01	0.02	0.02	0.03	0.03	0.04	0.05	0.05	0.06	0.07	0.08	0.09	0.10
	Restructuring Model	0.00	0.01	0.01	0.02	0.02	0.03	0.03	0.04	0.05	0.05	0.06	0.08	0.09	0.10	0.11
BB	Actual Default Rates	0.01	0.03	0.05	0.07	0.08	0.10	0.12	0.13	0.15	0.16	0.19	0.22	0.24	0.26	0.28
	Black-Cox Model	0.02	0.04	0.05	0.07	0.08	0.10	0.11	0.12	0.13	0.13	0.15	0.16	0.18	0.19	0.20
	Restructuring Model	0.01	0.03	0.05	0.06	0.08	0.10	0.12	0.13	0.15	0.16	0.19	0.22	0.24	0.26	0.28
B	Actual Default Rates	0.03	0.07	0.12	0.16	0.19	0.22	0.25	0.28	0.30	0.32	0.36	0.39	0.42	0.45	0.47
	Black-Cox Model	0.06	0.10	0.13	0.16	0.18	0.20	0.21	0.22	0.24	0.25	0.26	0.28	0.29	0.30	0.31
	Restructuring Model	0.03	0.08	0.12	0.16	0.19	0.22	0.25	0.28	0.30	0.32	0.36	0.39	0.41	0.44	0.46
C	Actual Default Rates	0.09	0.16	0.22	0.27	0.32	0.35	0.38	0.41	0.44	0.46	0.50	0.53	0.56	0.59	0.61
	Black-Cox Model	0.11	0.18	0.22	0.26	0.28	0.31	0.33	0.35	0.36	0.38	0.40	0.42	0.44	0.45	0.47
	Restructuring Model	0.09	0.16	0.22	0.27	0.32	0.35	0.38	0.41	0.44	0.46	0.50	0.53	0.55	0.58	0.60